Materials Research. 2025; 28:e20240594
DOI: https://doi.org/10.1590/1980-5373-MR-2024-0594

Effect of Low Solvent Concentration on the Rheological Behavior of Zirconia Ceramic Suspension and the Mechanical Properties of Sintered Parts

Giovanna Rubo de Rezende[a]*, Ítalo Leite de Camargo[b], Carlos Alberto Fortulan[a]

[a]Universidade de São Paulo (USP), Departamento de Engenharia Mecânica (EESC), Av. Trabalhador São Carlense, 400, São Carlos, SP, Brasil.
[b]Instituto Federal de Educação, Ciência e Tecnologia de São Paulo (IFSP), R. Primeiro de Maio, 500, Itaquaquecetuba, SP, Brasil.

Received: December 20, 2024; Revised: March 10, 2025; Accepted: April 21, 2025

Homogeneous and stable ceramic suspensions with high solids loading and low viscosity pose a significant challenge in vat photopolymerization additive manufacturing, once solid particles tend to increase viscosity. Instead, organic materials can contribute to decrease viscosity and post-sintering shrinkage. A base suspension was formulated using PEGDA along with dispersant DISPERBYK-111 (3 wt.% of the monomer powder), zirconia powder (40 vol.%), n-methyl-2-pyrrolidone (10% vol.), and a photoinitiator (2 wt.% of the monomer). The introduction of 10 vol.% solvent resulted in a 22.6% reduction in the suspension viscosity. The average post-sintering shrinkage measured 26.11% across all three dimensions. Sintered components exhibited an average density of 5.95 g/cm^3 and an average flexural strength of 256 ± 49 MPa. Additionally, the parts demonstrated anisotropic tribological behavior, low porosity and low surface roughness for polished (Ra 0.032) and untreated (Ra 0.33) surfaces. It was concluded that incorporating minimal amount of solvent into ceramic suspensions does not adversely affect their rheological and mechanical properties, while ensuring satisfactory surface quality of the sintered components.

Keywords: *Additive manufacturing, zirconia, digital light projection.*

1. Introduction

Additive manufacturing (AM) of ceramics through vat photopolymerization (VP) is a 3D printing technique that creates high-performance[1] and high-resolution objects[2] with a smooth surface finish, being able to achieve properties similar to those produced by traditional subtractive manufacturing[3]. The method is based on the computerized and gradual deposition of a resin loaded with ceramic powder in layers, transferring a digitized model to a mechanical system that produces the model, or "prints" it[4]. Once printing is complete, the resin is removed, and the residual powder undergoes sintering, thereby finalizing what is referred to as the indirect manufacturing process. In VP, a liquid photosensitive suspension is selectively cured within a vat using a light source[5], which triggers a polymerization chain reaction. This process allows the solidification of the pattern that corresponds to the object's cross-section, layer by layer, and can occur through stereolithography (SLA), digital light processing (DLP), or liquid crystal display (LCD)[6].

Some advantages of AM for ceramics over traditional methods include significant reduction in the need for tools and machinery, while maintaining the fidelity of dimension and details, even when producing geometrically complex and small parts[7]. Since ceramics have a high melting point, high susceptibility to thermal shock and low sinterability, completely consolidated and defect-free layers represent a challenge for direct AM of these materials[8-10] and, therefore, the indirect method has been adopted. Generally, the removal of organic material from ceramic printed parts is done thermally by degradation and decomposition. This method may require high temperatures for a long time, depending on the type of organic agent used (such as resin and solvents). However, as the amount of organic matter is relatively high, there may be partial vapor pressure in internal regions that are still impermeabilized or insufficiently connected to the external region, a condition that can generate cracks and delamination[10]. Therefore, it is recommended to design formulation with multiscale evaporative organic components because a component with a higher vapor pressure allows other volatiles to escape more easily, thus preventing defects in the manufacturing of parts[11]. It may be necessary to decrease the viscosity and improve the rheological properties of ceramic slurries, for example, by adding solvents to the ceramic suspension[12]. Solvents can also perform hybrid functions of lubricant, plasticizer and surfactant combined with multiscale removal. Typical ceramic slurry formulations for AM include a proportion of 10-20% solvents[13]. However, it's crucial to be mindful that the use of high vapor-pressure solvents can lead to warping and cracking, underscoring the importance of careful solvent selection[6].

The relevance of the selection of each element and its proportion in the formulation of ceramic suspensions for AM has been discussed in a paper[6] that emphasized that this selection is essentially based on the light adsorption and rheological properties, according to the type of 3D printing

*e-mail: giovana.rezende@usp.br

equipment, taking into account the wavelength of the available light source. Thus, the following factors were established as key to good rheological properties of ceramic suspensions for AM by VP: the powder particle size should be <0.5 μm for good sinterability; the specific surface area of the particle should be around $7 m^2/g$ for low viscosity; the binding agent and photoinitiator should be active at the wavelength of the light source provided by the AM equipment; dispersing agents should be added at a rate of 0.5 to 2.0% by weight relative to the powder content; solvents should correspond to up to 20% by volume relative to the powder content[14]. Despite these recommendations, the use of solvent-free suspensions or with a minimal proportion of solvent (10% by volume) has been recommended to reduce shrinkage and improve the geometry of the final part, without significantly interfering with the rheological properties of the suspension[15-19].

Among the ceramic materials used to produce parts with AM technology, zirconia (ZrO_2) stands out for its high hardness, resistance to bending and fracture, excellent ionic conductivity, thermal and chemical stability, biocompatibility and corrosion resistance[20]. To overcome problems related to the final quality of parts produced in zirconia ceramics by AM, measures have been adopted such as: use of dense zirconia such as 3Y-TZP in high solid loading suspensions[16]; adjustments to the ideal power of the photopolymerizing light source and energy flow[15]; a combination of AM techniques with traditional techniques to improve mechanical performance[2], and to reduce the amount of solvents in order to improve stability of rheological properties as well as for reducing shrinkage[15,17,18].

The effect of the composition of the ceramic suspension has been widely studied not only on its rheological properties but also on the mechanical behavior of the final part[2,3,6,12,15,17,21]. In this sense, feedstock formulation is a major factor in obtaining the desired mechanical properties. A preliminary study carried out by this research group[15] used a high amount of solvents (exceeding 30%) to prepare a 3Y-TZP suspension which, after debinding and sintering at 1500 C for two hours, produced parts with an average flexural strength of 337 MPa. However, the high volume of organics resulted in a large linear shrinkage exceeding 34%. Subsequent studies based on solvent-free suspensions[16,22] were performed to overcome this downside, reducing shrinkage to about 25%. Nevertheless, 3Y-TZP with limited average flexural strength (<200 MPa) was obtained, indicating that the solvent may have benefits beyond reducing suspension viscosity. Thus, in this work, formulations with a minimal amount of solvent will be explored.

2. Materials and Methods

A preliminary test was conducted to select the solvent used in this work. Thus, a base formulation composed of a monomer (PEGDA 250, Sigma Aldrich, USA) and 2 wt% of a photoinitiator (phenylbis (2,4,6-trimethylbenzoyl) phosphine oxide, Sigma Aldrich, USA) was prepared in a magnetic stirrer for 4 hours. Subsequently, 10 vol% of different solvents (methyl alcohol, benzyl alcohol, camphor, ethylene glycol, ethyl alcohol, isopropyl alcohol, n-methyl-2-pyrrolidone, and polyethylene glycol) were incorporated. Each prepared formulation was poured into the vat of the 3D printer and subjected to different light exposure times (up to 10 seconds) to check the effect of the solvent on the layer formation. All solvents considered, except n-methyl-2-pyrrolidone, did not form a uniform layer, presenting regions with incomplete polymerization and a gelatinous appearance. The same test was repeated 7 days after the preparation of the mixtures to verify whether they could be used after storage. The n-methyl-2-pyrrolidone, which has already been successfully used in a preliminary work by this research group[15], produced uniform layers, even after 7 days of storage, and thus, it was selected as the solvent in the development of ceramic suspensions in this study.

2.1. Production of ceramic suspensions for characterization

To investigate the impact of low solvent content (10% by volume of the monomer) on the rheological behavior of the ceramic suspension, a formulation was produced containing 3Y-TZP zirconia powder with a specific surface area of $16 \pm 3 m^2/g$ at 15% by total volume (TZ-3Y-E, Tosoh Corporation, Japan), poly (ethylene glycol) diacrylate monomer (PEGDA 250, Sigma Aldrich, USA), DISPERBYK-111 dispersant (BYK-Chemie, Germany) at 3% by weight of the monomer, n-methyl-2-pyrrolidone (Synth, Labsynth, São Paulo) at 10% by volume of the monomer. The viscosity of this formulation was compared to previous results[6], using a solvent-free formulation containing the same elements in the same proportions.

The rheological behavior of the formulations was assessed through a viscosity test performed at room temperature using a rotational viscometer (DV2T Extra, Brookfield).

2.2. Suspension preparation for AM

A suspension containing 3Y-TZP zirconia powder at 40% by total volume, PEGDA 250, DISPERBYK-111 dispersant at 3% by weight of the monomer, n-methyl-2-pyrrolidone at 10% by volume of the monomer and photoinitiator phenylbis (2,4,6-trimethylbenzoyl) phosphine oxide (PPO, Sigma Aldrich, USA) was produced. The preparation of the suspension started with mixing the monomer, dispersant and solvent together. Next, the ceramic powder and the photoinitiator were gradually added into the mixture. The suspension was then homogenized in a ball mill for 24 h to break up any agglomerates, as suggested in a related work[16].

2.3. Production of parts by AM and sintering.

Six identical green parts with a layer thickness of 25 μm were produced using a customized top-down AM machine[23]. The layer thickness was chosen based on a recommendation[8] suggesting that it should be set within an appropriate range, typically between 15 μm and 100 μm. The lower limit is generally determined by the capabilities of the SL apparatus, while the upper limit results from a balance between the required surface resolution and curing depth[8]. After being produced, the pieces were washed with isopropyl alcohol and dried in an oven at 100°C for 12 hours. The process of burning the organic components of the pieces occurred by gradual heating from 350°C to 600°C[17,19] and, subsequently, the pieces were sintered at 1500ºC for 2 hours in the box furnace, a process in which porosity was reduced,

increasing their density. The final pieces were then cleaned and finished. The samples were subjected to post-sintering shrinkage analysis (measurements by caliper), density (Archimedes' principle applied with a mass measurement resolution of 0.01 mg), mechanical bending test, wear resistance ("pin-on-disc" test), porosity and surface roughness analysis (SEM and confocal microscopy respectively). A case study was conducted to evaluate the manufacturing process of dental brackets, focusing on the friction force between the groove surface of the bracket and the arch wire.

2.4. Mechanical bending test

A universal mechanical testing machine (Bionix, MTS 370.02) equipped with a 15 kN load cell operating at the speed of 1.5 mm/min at 20°C was utilized. The bending test based on ASTM C1161-02c[24] was performed bar-shaped specimens measuring 25 x 2.0 x 1.5 mm (post-sintering dimensions) at 3 points within the distance of 20 mm between the supports. The test specimens were digitally designed in the dimensions of 34 x 2.7 x 2 mm in green state, anticipating a contraction of 26%[16].

An additional set of tests was performed on flexural samples manufactured from a suspension prepared using a planetary mixer (Speed Mixer DAC 1100-1 FVZ, Hauschild) at 1600 rpm for 4 minutes instead of using the ball mill.

2.5. Wear resistance according to the direction of layer deposition

To investigate the influence of layer deposition direction on zirconia produced by AM, the "pin-on-disc" test was conducted according the ASTM G99-05 standard[25]. The pins were manufactured with 50 µm layer thickness and were underwent to the exposure time of 10s/layer. Such parts were manufactured in two distinct printing directions: perpendicular and parallel to the shear direction. After manufacturing, the pins were sintered at 1500ºC for 2 hours and fixed to the metal support with adhesive (AralditeTM, Tekbond, SP, Brazil) which cured over 24 hours followed by heat treatment for 2 hours at 100ºC. The experimental conditions were as follows:

- 10 N of applied load under atmospheric humidity between 45 and 55%;
- sliding of the zirconia pin over an alumina disc (Sain Gobain Ceramics / Brazil) purity >99%, flat surface grinding, Ra 0.25 +/- 0.08 µm;
- sliding speed of 1 m/s;
- traveled distance of 500 m in each mass loss measurement stage;
- 1.5 km of total distance traveled.

A standard counter-test was performed with a 5 mm diameter zirconia ball, HV10 1250, (Tosoh YTZ® Grinding medium), fracture toughness of 6,0 MPa.m^{0,5}, firmly fixed to a metal support and tested under the same experimental conditions as for the AM pins.

2.6. Porosity

Printed samples with layers of 50 µm, 40 µm, 25 µm and 10 µm thickness were examined by SEM to evaluate the presence of pores and cracks. Each piece was embedded in epoxy resin and polished with sandpaper of 150, 320, 600, 1200, 2000 grit consecutively. Each sandpaper was used for 5 minutes and its surface was rotated 90º at every sandpaper change. After polishing, the samples were heat treated for 6 min/air at a temperature of 1313°C (T_{etch}), with heating rate of 10°C/min according to the Equation 1[19].

$$T_{etch} = T_{sint} * 0.875 + 100 \quad (1)$$

where T_{etch} is the thermal attack temperature (°C), and T_{sint} is the sintering temperature (°C). The samples were metallized with gold and observed under a scanning electron microscope. (MEV - JSM7500 F, Jeol) regarding the presence of porosities.

2.7. Roughness

Other samples produced with 25µm layer thickness were examined under a confocal microscope (Olympus Lext 3D measuring laser microscope OLS4100) to measure surface roughness (Ra) at 20x magnification.

In this test, two groups were analyzed: samples without additional preparation (as-sintered) and after polishing with 150, 320, 600, 1200, and 2000 grit sandpaper, followed by 6 µm and 1 µm Diamond Polishing Paste, with each step lasting 5 minutes.

3. Results and Discussion

3.1. Effect of solvent on viscosity

The results of the effect of the solvent on the viscosity of the ceramic suspension can be seen in Figure 1, where the viscosity curves are presented. At all shear rate points at which viscosity was measured, the formulation containing 10% by volume of n-methyl-2-pyrrolidone was less viscous. For comparison purposes, a shear rate of 30s^{-1} is considered standard in the literature[6,16,21]. At this rate, the viscosity of the solvent-containing formulation was 22.6% lower than that of the solvent-free formulation. Since ceramic formulations with high solid loading are very viscous, pyrrolidone, even at a low concentration of 10% by volume, significantly reduced the viscosity of the formulation, facilitating the formation of uniform suspension layers.

3.2. Shrinkage and density of sintered parts

The shrinkages observed in the average dimensions of the green parts after sintering were 26.02% in the length direction,

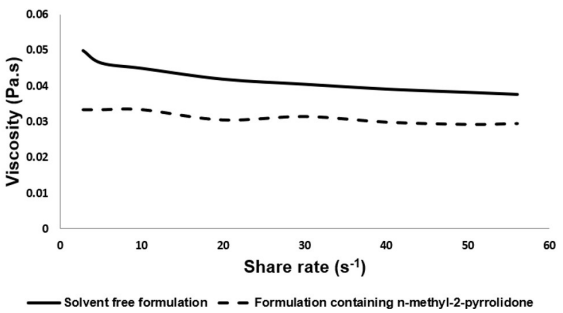

Figure 1. Influence of solvent on the viscosity of the ceramic formulation.

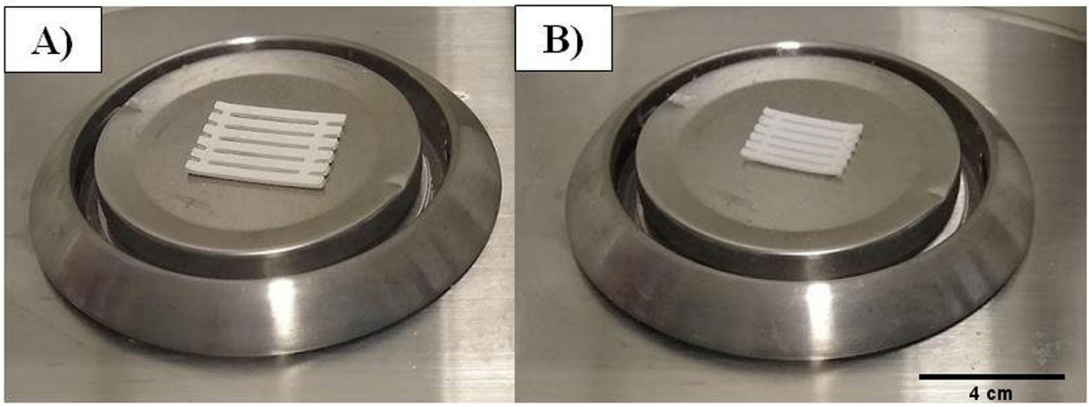

Figure 2. Shrinkage of test specimens: A) before sintering; B) after sintering.

26.25% in the width; and thickness represented 26.33% in the diameter, 26.25% in the width direction and 26.54% in the thickness direction. These results are in consistent with findings from the literature that examined suspensions with similar formulations, but free of solvents[16,22]. Additionally, the shrinkage measured here is even lower than the shrinkage reported for formulations that contain solvents[15].

The shrinkage of the test specimens is illustrated in Figure 2. The average density of the sintered specimens was measured at 5.95 g/cm^3. Considering the theoretical density[26] of TZ-3Y-E zirconia at 6.12g/cm^3, the relative density of these specimens is calculated to be 97.14%. This result is consistent with findings from previous publications[15,27]. This outcome confirms that the formulation used in this study produced ceramic bodies with high-density after sintering, which is crucial for maintaining the stability of the tetragonal phase of zirconia ceramics[26].

3.3. Mechanical bending test

The average flexural strength was 256 ± 49 MPa. Some researchers[22] observed approximately 150 MPa of flexural strength in specimens with 100 µm layer thickness produced with the same formulation, but without solvent. Other authors[15], in turn, varying the amount of n-methyl-2-pyrrolidone solvent between 50% and 79% by volume in the formulation found an average flexural strength of 337 MPa in test specimens produced with 50 µm thick layers. This apparent advantage in the use of high solvent concentration, on the other hand, was responsible for high shrinkage of the parts (from 34% to 36%)[15] compared to our results, where a minimum amount of solvent was used. In fact, the approximately 26% shrinkage observed here is comparable to the results obtained with solvent-free formulations[16].

In this study, the breaking point in the flexural test occurred at the interface between the layers. This finding is consistent with observations made by other authors[16,28]. It was suggested[16] that the decrease in layer thickness associated with the addition of plasticizers to the formulation could increase flexural strength. In fact, flexural strength was higher in this study compared to that of the aforementioned authors[16]. However, the reduction in the thickness of the deposition layer was not enough to prevent the failure at the interface. An important consideration is that a balance between layer thickness and solvent quantity was identified, resulting in intermediate flexural strength values that fall between those reported by previous researchers.

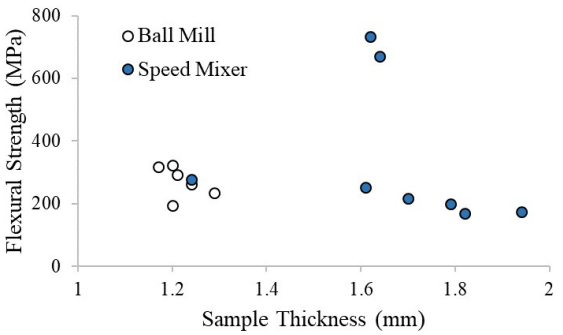

Figure 3. Flexural strength as a function of sample thickness for the two suspension preparation protocols used.

Figure 3 shows the variation in flexural strength versus sample thickness for the two suspension preparation protocols used. Some samples from the planetary speed mixer presented remarkable flexural strength, obtaining a maximum value that exceeds 730 MPa. However, such samples presented an average flexural strength of 336 ± 229 MPa, showing a standard deviation much larger than the samples obtained from the suspension prepared in the ball mill, which may be associated with the excellent homogenization provided by the ball mill already reported in related works[16,17,19], in addition to the greater variation in sample thickness in the samples in the planetary mixer, since larger samples are more likely to present defects.

3.4. Wear resistance according to the direction of layer deposition

The results of the pin-on-disk test regarding the mass loss of the ball and pins produced in the perpendicular and parallel directions are shown in Figure 4.

The pin manufactured with layers oriented perpendicular to the abrasive disc exhibited the highest peak mass loss within the first 500 m. This mass loss was over 2.5 times greater than that experienced by the pin produced with layers parallel to the disc. As the wear test continued, both pin types showed a

tendency towards stabilization in mass loss. The zirconia ball exhibited even greater mass losses, and it was impossible to measure the mass loss after 1500 m. By the end of the 1500 m test, the pin produced with perpendicular layers displayed a volumetric loss rate 53% higher than that of the pin with parallel layers. Table 1 presents the volumetric loss rates for both the pins and the ball during the first 1500 m traveled.

Although the initial area of the ball is smaller than the area of the pin, it has been found that the AM process maintains exceptional wear characteristics for the zirconia when following the concept of design for additive manufacturing (DFAM), specifically in relation to the friction force acting tangentially to the deposited surface. The evaluation of the friction force between the pins and the ball revealed that the friction coefficient tends to stabilize at the average value of 0.6 for all samples. However, this value was only reached by the pin produced with layers parallel to the disc after 1500 m of testing. This result confirms that this was the most wear-resistant sample. In contrast, the ball exhibited a friction coefficient of 0.54 already in the first 500 m of the course, being the least wear-resistant sample.

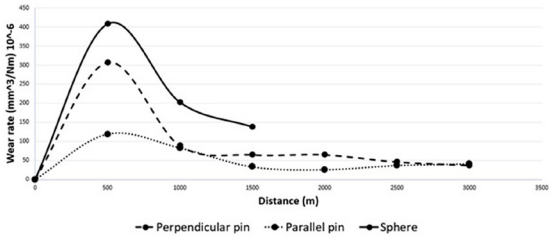

Figure 4. Loss of mass along the distance traveled by the pins and the sphere.

3.5. Porosity

Figure 5 shows the images generated by SEM with 10x magnification to evaluate the presence of pores and cracks in samples with different layer deposition thicknesses.

The SEM showed that the surfaces were free of cracks and had no porosity detected for the samples with 50 µm, 40 µm and 10 µm layer thickness. The surface of the sample produced with 25 µm layer thickness showed small, uniform and homogeneous pores, the largest of which was around

Table 1. Volumetric loss rate of samples in the first 1500 m traveled.

Sample	Loss rate in the first 1500 m	Relative loss rate (%)
Perpendicular layers pin	0.46. 10^{-5}	153
Paralel layers pin	0.3. 10^{-5}	100
Sphere	0.41. 10^{-5}	135

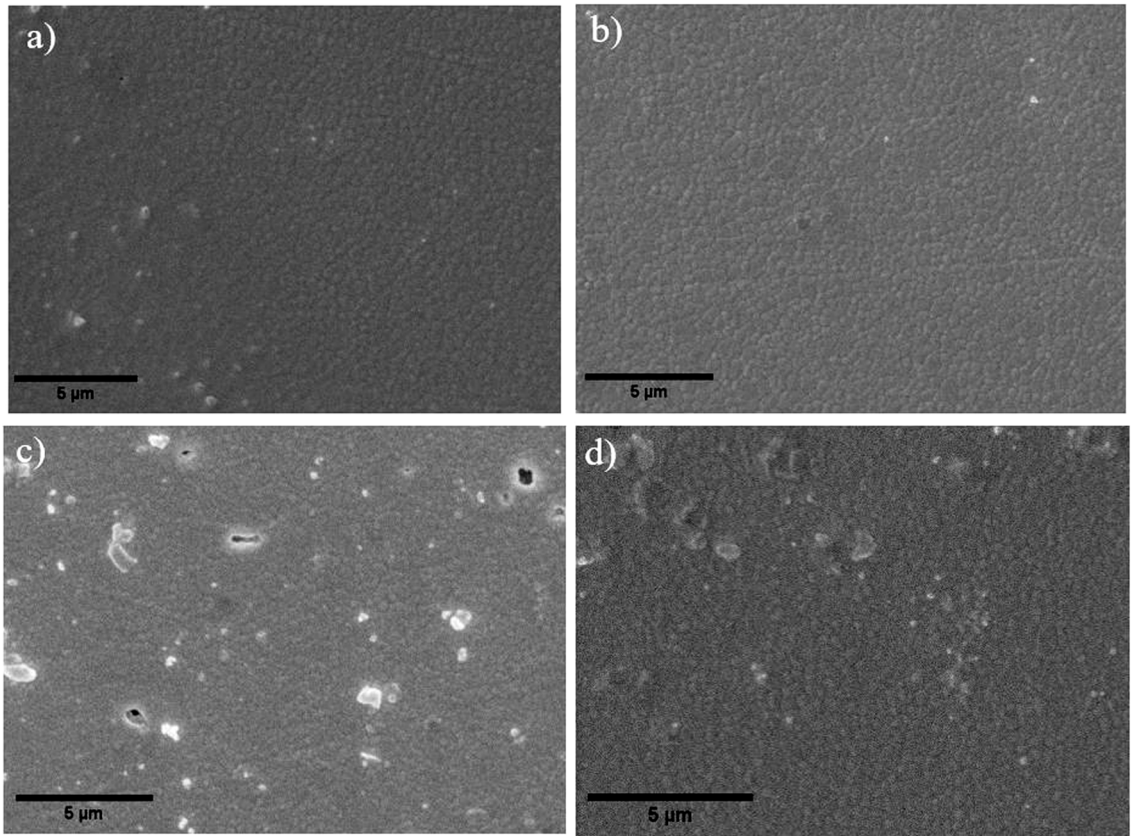

Figure 5. SEM images (10x) of samples with layer thicknesses of: a) 50 µm; b) 40 µm; c) 25 µm and d) 10 µm.

0.3 µm. This sample may have presented an atypical and non-representative behavior, which suggests that the layer thickness does not interfere with the surface porosity in relation to the layer stacking direction. Furthermore, the bonding between layers was so uniform in all samples subjected to SEM analysis that it was not possible to identify the boundaries between layers in the cross section of the parts after the sanding and polishing process, unlike what was observed by other authors[22,29,30]. Given these observations, the initial hypothesis that layers with thicknesses ≤ 25 µm would promote greater adhesion between layers was not confirmed by this study.

Figure 6 shows the SEM image of the fracture surface of a printed sample with a layer thickness of 25 µm which was subjected to the bending test. The fracture surface showed low porosity (0.15%) and no cracks, with small uniform and homogeneous pores, the largest of which measured 0.6 µm. A SEM analysis of a zirconia dental implant produced with the DLP technique in AM with 30 µm layer thickness[31] evidenced, in addition to cracks, microporosities ranging in size from 196 nm to 3.3 µm, therefore, more than 5 times larger than the largest pore on the fracture surface found in the sample in Figure 6.

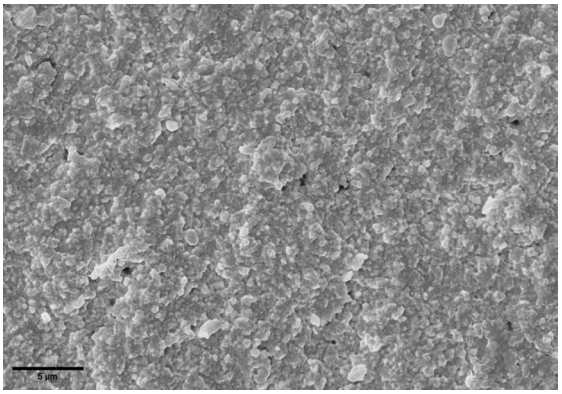

Figure 6. SEM image of the fracture surface of a sample produced with layer thickness of 25µm.

The explanation given for the occurrence of cracks and pores of those dimensions was the possible evaporation of the solvent from the ceramic formulation on the exposed surface during printing that occurs before the deposition of the next layer, which can cause differential shrinkage after sintering, causing fissures and porosities. This explanation endorses the importance of choosing the appropriate solvent for the manufacture of zirconia ceramic formulations.

3.6. Roughness

The average value of surface roughness (Ra) measured by confocal microscopy in samples manufactured with 25 µm layer thickness and without polishing was 0.33 µm. Figure 7 shows the confocal microscopy image obtained from the surface subjected to roughness analysis.

This obtained roughness was much lower than the value found by other authors in zirconia parts (TZ-3YS-E) produced by DLP (1.59 µm)[31]. Surface roughness becomes particularly relevant when the manufactured part will have a biological use, as in the case of intraosseous implants, prostheses and intraoral accessories, because they come into contact with bacterial contamination pathways that can favor the growth of biofilms on their surfaces. Although a classic publication[32] found that surfaces with roughness values above 0.2 µm are more predisposed to the adhesion of microorganisms, the authors emphasized that roughness is not the only parameter to be taken into consideration in this analysis, since on smooth surfaces, as long as they present high surface energy and wettability, there may also be deposition of bacterial biofilm[33].

Figure 8 shows confocal microscopy images of the surface of a zirconia part manufactured by AM with a layer

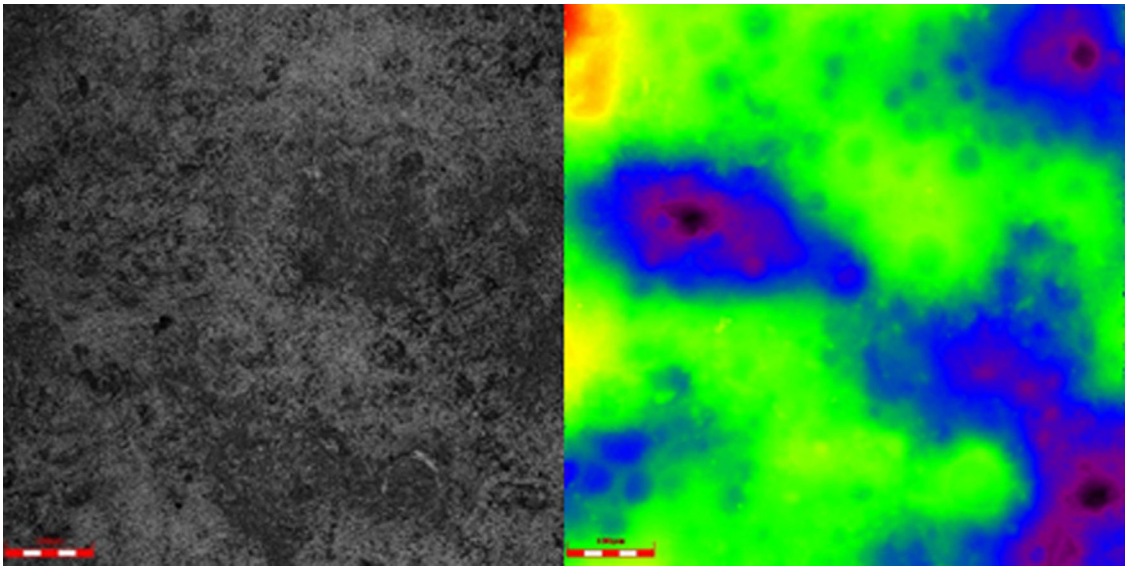

Figure 7. Confocal microscopy of the surface of a sample produced with a layer thickness of 25 µm (scale: 100 µm). Both images refer to the same region of the part.

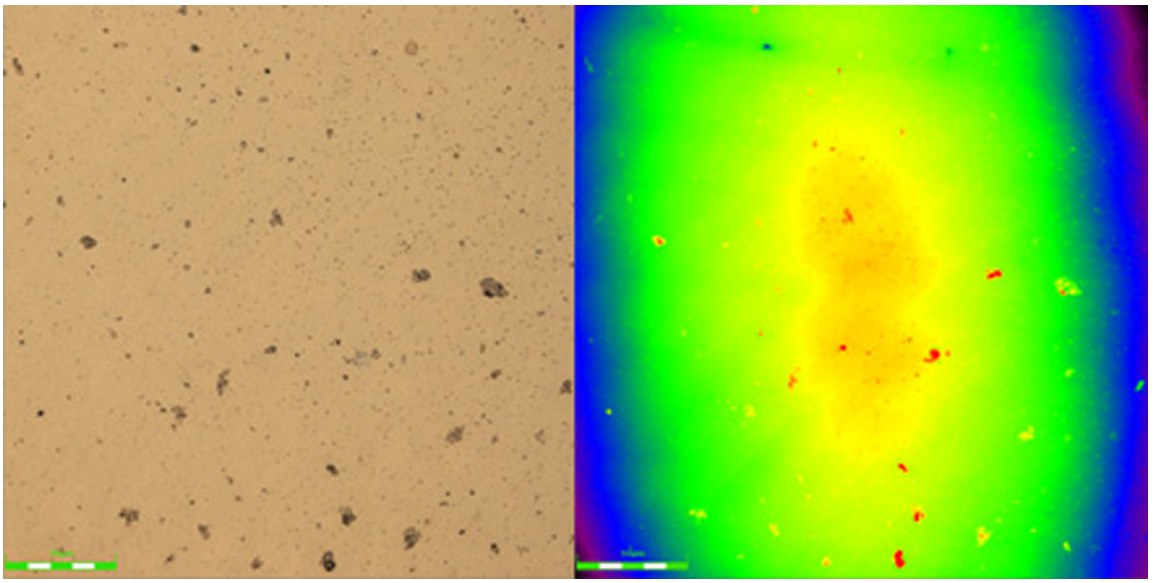

Figure 8. Confocal microscopy of the polished surface of a zirconia sample. Both images refer to the same region of the sample (scale value: 50µm).

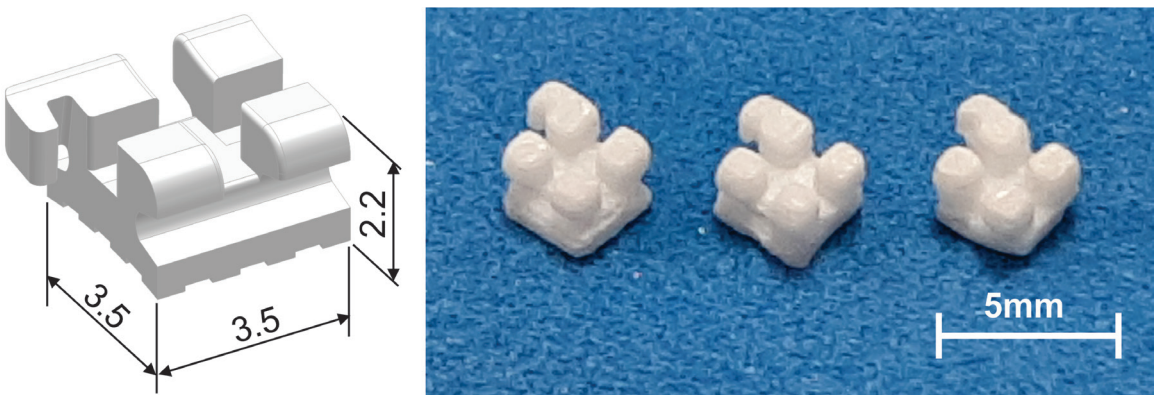

Figure 9. Case study of 3Y-TZP dental bracket, a) model and b) printed and sintered samples.

thickness of 25 µm after polishing. The surface roughness of this part showed an average value of 0.032 µm, therefore six times lower than the value above which bacterial adhesion can be expected. This demonstrates that, although AM of zirconia, nowadays, is not capable of manufacturing parts with roughnesses smaller than 0.2 µm, polishing the surfaces produces surfaces smooth enough to avoid this accumulation.

3.7. Case study

Printed samples of dental brackets are shown in Figure 9, with a) depicting the 3D model and b) displaying the printed and sintered samples. The printing setup was 50 µm for thickness layer and 20s of exposition time to light.

The average coefficient of friction presented by the stainless-steel bracket was 0.19, while the coefficient of friction generated by the zirconia bracket presented an average value of 0.37 (1.94 times higher). The discussion of these results was hampered by the lack of data in the literature evaluating friction between zirconia brackets and orthodontic wires. However, some studies have shown that, in commercial zirconia brackets, although the friction generated is slightly greater in relation to the stainless-steel bracket, this friction is still considered low, not significantly interfering with orthodontic mechanics[34,35], which makes its use suitable for this function.

4. Conclusions

The addition of a minimum amount of solvent to the zirconia ceramic formulation yielded favorable results, including a significant reduction in the viscosity of the formulation, which facilitated the formation of uniform layers during the AM process; maintenance of post-sintering shrinkage within the expected 26%, representing an improvement over previous work by the same team, providing higher flexural strength compared to solvent-free formulations. In addition,

obtaining parts almost free of porosity and cracks confirms that reducing the proportion of solvent and the properties of the chosen solvent are important factors for improving the quality of the sintered part.

It was concluded that the direction of layer deposition influences the anisotropic behavior of the final product. Specifically, the direction with the greatest wear resistance was found to be parallel to the abrasive disc. This conclusion is significant for guiding the manufacturing of parts based on their intended functions.

The SEM analysis revealed that the layers were well consolidated, making the boundaries between the layers indistinguishable. These findings were attributed to the careful selection of components and the precise adjustments made while producing the suspension in the specified proportions.

The low surface roughness values observed on both polished and untreated surfaces after the sintering process are particularly significant when a smooth surface finish is essential, which is especially important for parts that will be used in environments rich in bacteria, such as the oral cavity.

5. Acknowledgments

This study was funded by the State of São Paulo Research Foundation (FAPESP), project number 2021/12612-7 and by the "National Council for Scientific and Technological Development" (CNPq), grant number 307143/2022-8.

6. References

1. Wang J. A novel fabrication method of high strength alumina ceramic parts based on solvent-based slurry stereolithography and sintering. Int J Precis Eng Manuf. 2013;14(3):485-91. http://doi.org/10.1007/s12541-013-0065-3.
2. Xing H, Zou B, Li S, Fu X. Study on surface quality, precision and mechanical properties of 3D printed ZrO2 ceramic components by laser scanning stereolithography. Ceram Int. 2017;43(18):16340-47. http://doi.org/10.1016/j.ceramint.2017.09.007.
3. Borlaf M, Szubra N, Serra-Capdevila A, Kubiak WW, Graule T. Fabrication of ZrO2 and ATZ materials via UV-LCM-DLP additive manufacturing technology. J Eur Ceram Soc. 2020;40(4):1574-81. http://doi.org/10.1016/j.jeurceramsoc.2019.11.037.
4. Trombetta R, Inzana JA, Schwarz EM, Kates SL, Awad HA. 3D printing of Calcium phosphate ceramics for bone tissue engineering and drug delivery. Ann Biomed Eng. 2017;45(1):23-44. http://doi.org/10.1007/s10439-016-1678-3.
5. Lovo JFP, Camargo IL, Erbereli R, Morais MM, Fortulan CA. Vat photopolymerization additive manufacturing resins: analysis and case study. Mater Res. 2020;23(4):e20200010. http://doi.org/10.1590/1980-5373-mr-2020-0010.
6. Camargo IL, Morais MM, Fortulan CA, Branciforti MC. A review on the rheological behavior and formulations of ceramic suspensions for vat photopolymerization. Ceram Int. 2021;47(9):11906-21. http://doi.org/10.1016/j.ceramint.2021.01.031.
7. Levy GN, Schindel R, Kruth JP. Rapid manufacturing and rapid tooling with Layer Manufacturing (LM) technologies, state of the art and future perspectives. CIRP Ann. 2003;52(2):589-609. http://doi.org/10.1016/S0007-8506(07)60206-6.
8. Fiume E, Coppola B, Montanaro L, Palmero P. Vat-photopolymerization of ceramic materials: exploring current applications in advanced multidisciplinary fields. Front Mater. 2023;10:1242480. http://doi.org/10.3389/fmats.2023.1242480.
9. Ngo TD, Kashani A, Imbalzano G, Nguyen KTQ, Hui D. Additive manufacturing (3D printing): A review of materials, methods, applications and challenges. Compos, Part B Eng. 2018;143:172-96. http://doi.org/10.1016/j.compositesb.2018.02.012.
10. Galante R, Figueiredo-Pina CG, Serro AP. Additive manufacturing of ceramics for dental applications: A review. Dent Mater. 2019;35(6):825-46. http://doi.org/10.1016/j.dental.2019.02.026.
11. Johansson E, Lidström O, Johansson J, Lyckfeldt O, Adolfsson E. Influence of resin composition on the defect formation in alumina manufactured by stereolithography. Materials. 2017;10(2):138. http://doi.org/10.3390/ma10020138.
12. Wang JC, Dommati H. Fabrication of zirconia ceramic parts by using solvent-based slurry stereolithography and sintering. Int J Adv Manuf Technol. 2018;98(5-8):1537-46. http://doi.org/10.1007/s00170-018-2349-3.
13. Griffith ML, Halloran JW. Freeform fabrication of ceramics via stereolithography. J Am Ceram Soc. 1996;79(10):2601-08. http://doi.org/10.1111/j.1151-2916.1996.tb09022.x.
14. Gonzalez P, Schwarzer E, Scheithauer U, Kooijmans N, Moritz T. Additive manufacturing of functionally graded ceramic materials by stereolithography. J Vis Exp. 2019; e57943. http://doi.org/10.3791/57943.
15. Amaral LB, Paschoa JLF, Magalhães DV, Foschini CR, Suchicital CTA, Fortulan CA. Preliminary studies on additive manufacturing of over 95% dense 3Y zirconia parts via digital imaging projection. J Braz Soc Mech Sci Eng. 2020;42(1):75. http://doi.org/10.1007/s40430-019-2157-1.
16. Camargo IL, Erbereli R, Taylor H, Fortulan CA. 3Y-TZP DLP additive manufacturing: solvent-free slurry development and characterization. Mater Res. 2021;24(2):e20200457. http://doi.org/10.1590/1980-5373-mr-2020-0457.
17. Camargo IL, Erbereli R, Fortulan CA. Additive manufacturing of electrofused mullite slurry by digital light processing. J Eur Ceram Soc. 2021;41(14):7182-88. http://doi.org/10.1016/j.jeurceramsoc.2021.07.005.
18. Hsu H-J, Lee S-Y, Jiang C-P, Lin R. A comparison of the marginal fit and mechanical properties of a zirconia dental crown using CAM and 3DSP. Rapid Prototyping J. 2019;25(7):1187-97. http://doi.org/10.1108/RPJ-03-2018-0053.
19. Camargo IL, Erbereli R, Lovo JFP, Fortulan R, Fortulan CA. Digital light processing additive manufacturing of in situ mullite-zirconia composites. J Eur Ceram Soc. 2022;42(13):6025-32. http://doi.org/10.1016/j.jeurceramsoc.2022.06.042.
20. Zhang X, Wu X, Shi J. Additive manufacturing of zirconia ceramics: a state-of-the-art review. J Mater Res Technol. 2020;9(4):9029-48. http://doi.org/10.1016/j.jmrt.2020.05.131.
21. Li X, Zhong H, Zhang J, Duan Y, Bai H, Li J, et al. Dispersion and properties of zirconia suspensions for stereolithography. Int J Appl Ceram Technol. 2020;17(1):239-47. http://doi.org/10.1111/ijac.13321.
22. Camargo IL, Erbereli R, Lovo JFP, Fortulan CA. DLP additive manufacturing of ceramics: photosensitive parameters, thermal analysis, post-processing, and parts characterization. In: 11th Brazilian Congress on Manufacturing Engineering, 2021 May 24-26; Curitiba. Rio de Janeiro: ABCM; 2021. https://doi.org/10.26678/ABCM.COBEF2021.COB21-0106.
23. de Rezende GR, Fortulan CA. Design, construction, and validation of a VAT top-down printer for ceramic additive manufacturing. Cerâmica. 2025;71:eCWBA5731.
24. ASTM: American Society for Testing and Materials. ASTM C1161-02c: standard test method for flexural strength of advanced ceramics at ambient temperature. West Conshohocken: ASTM; 2017.
25. ASTM: American Society for Testing and Materials. ASTM G99-05: standard test method for wear testing with a pin-on-disk apparatus. West Conshohocken: ASTM; 2016.
26. Tadokoro SK, Muccillo ENS. Zircônia tetragonal policristalina. Parte II: microestrutura e resistividade elétrica. Cerâmica.

2001;47(302):100-8. http://doi.org/10.1590/S0366-69132001000200007.

27. Camargo IL, Verza JR, Garcia J, Di Federico D, Fortulan CA, Luz AP. Fused filament fabrication of partially stabilized zirconia (3Y-TZP) parts. Mater Lett. 2024;355:135510. http://doi.org/10.1016/j.matlet.2023.135510.
28. Shen M, Zhao W, Xing B, Sing Y, Gao S, Wang C, et al. Effects of exposure time and printing angle on the curing characteristics and flexural strength of ceramic samples fabricated via digital light processing. Ceram Int. 2020;46(15):24379-84. http://doi.org/10.1016/j.ceramint.2020.06.220.
29. Abualsaud R, Abussaud M, Assudmi Y, Aljoaib G, Khaled A, Alalawi H, et al. Physiomechanical and surface characteristics of 3D-printed zirconia: an in vitro study. Materials. 2022;15(19):6988. http://doi.org/10.3390/ma15196988.
30. Osman R, Alharbi N, Wismeijer D. Build angle: does it influence the accuracy of 3D-Printed dental restorations using digital light-processing technology? Int J Prosthodont. 2017;30(2):182-88. http://doi.org/10.11607/ijp.5117.
31. Osman RB, van der Veen AJ, Huiberts D, Wismeijer D, Alharbi N. 3D-printing zirconia implants; a dream or a reality? An in-vitro study evaluating the dimensional accuracy, surface topography and mechanical properties of printed zirconia implant and discs. J Mech Behav Biomed Mater. 2017;75:521-28. http://doi.org/10.1016/j.jmbbm.2017.08.018.
32. Bollenl CML, Lambrechts P, Quirynen M. Comparison of surface roughness of oral hard materials to the threshold surface roughness for bacterial plaque retention: a review of the literature. Dent Mater. 1997;13(4):258-69. http://doi.org/10.1016/S0109-5641(97)80038-3.
33. Yuan C, Wang X, Gao X, Chen F, Liang X, Li D. Effects of surface properties of polymer-based restorative materials on early adhesion of *Streptococcus mutans* in vitro. J Dent. 2016;54:33-40. http://doi.org/10.1016/j.jdent.2016.07.010.
34. Keith O, Kusy RP, Whitley JQ. Zirconia brackets: an evaluation of morphology and coefficients of friction. Am J Orthod Dentofacial Orthop. 1994;106(6):605-14. http://doi.org/10.1016/S0889-5406(94)70085-0.
35. Tanne K, Matsubara S, Hotei Y, Sakuda M, Yoshida M. Frictional forces and surface topography of a new ceramic bracket. Am J Orthod Dentofacial Orthop. 1994;106(3):273-78. http://doi.org/10.1016/S0889-5406(94)70047-8.